

# METHODS FOR THE MICROFABRICATION OF MAGNESIUM

Melissa Tsang<sup>1</sup>, Florian Herrault<sup>2</sup>, Richard H. Shafer<sup>2</sup>, and Mark G. Allen<sup>2</sup>

<sup>1</sup>School of Biomedical Engineering, Georgia Institute of Technology, USA

<sup>2</sup>School of Electrical and Computer Engineering, Georgia Institute of Technology, USA

## ABSTRACT

The mechanical and electrochemical properties of magnesium are favorable for biomedical and energy storage applications. However, magnesium microfabrication has been limited to submicron-thick film technologies (i.e., sputtering or evaporation). This paper presents three magnesium microfabrication approaches for thicknesses greater than 10  $\mu\text{m}$ : 1) laser-cutting and 2) chemical etching of 70- $\mu\text{m}$ -thick commercial magnesium foil; and 3) through-mold electroplating of magnesium from non-aqueous solution. The fabrication technologies are compared on minimum feature size, morphology, uniformity, composition and electrical resistivity. Preliminary results confirmed that the 50- $\mu\text{m}$ -thick electroplated material composition compared favorably with commercial magnesium foil. The measured electrical resistivities of commercial and electrodeposited magnesium were 5.3  $\mu\Omega\cdot\text{cm}$  and 8.7  $\mu\Omega\cdot\text{cm}$ , respectively. Thick magnesium microstructures can be fabricated through several means to serve a broad range of MEMS-based applications.

## INTRODUCTION

The element magnesium (Mg) has a variety of desirable mechanical, electrochemical, and biomedical properties. Specifically, magnesium exhibits a high modulus-to-density ratio, comparable to that of aluminum [1]. Further, the electrochemical activity and biodegradable nature of magnesium has been explored for energy storage applications [2] and biomedical implants [3]. However, current methods of fabricating and patterning this material are incompatible with traditional MEMS fabrication techniques. This paper reports both additive and subtractive approaches to magnesium

microfabrication, with the ultimate goal of incorporating this important element into MEMS structures.

Traditional ways of integrating metals into MEMS processes include sputtering, evaporation, and electrodeposition. The sputtering of magnesium thin films has been investigated for corrosion resistant surface coatings and biodegradable electronics [3, 4]. When relatively thick films are desired, electrodeposition becomes attractive; however, the high electrochemical potential of magnesium (-2.4 V against hydrogen) makes it challenging to electrodeposit from aqueous solutions [2]. Other approaches to integration of metals include micromachining directly onto metal foils and integration of these foils with other MEMS. D.M. Allen *et al.* described a process for photochemical etching of 250- $\mu\text{m}$ -thick magnesium foils with approximately 300- $\mu\text{m}$ -wide lines and millimeter-scale spacing [6], but no MEMS integration was investigated. Boutry *et al.* fabricated magnesium-based RLC resonators using electric discharge machining (EDM) of 3-mm-thick magnesium sheet with a feature width of 1 cm and a gap of 0.6 mm [7]. Also, the electrodeposition of magnesium films from non-aqueous solutions has been demonstrated for hydrogen storage applications, targeting fine grain and porous deposits, but no micropatterning was performed [8].

We have previously demonstrated the laser micromachining of metals [9], as well as the electrodeposition of electrochemically-active aluminum from non-aqueous solutions [10]. This paper presents the application of laser micromachining, chemical etching, and through-resist electrodeposition technologies to the magnesium microfabrication at thicknesses on the order of tens of microns, and illustrates some of the advantages and limitations of these processes.

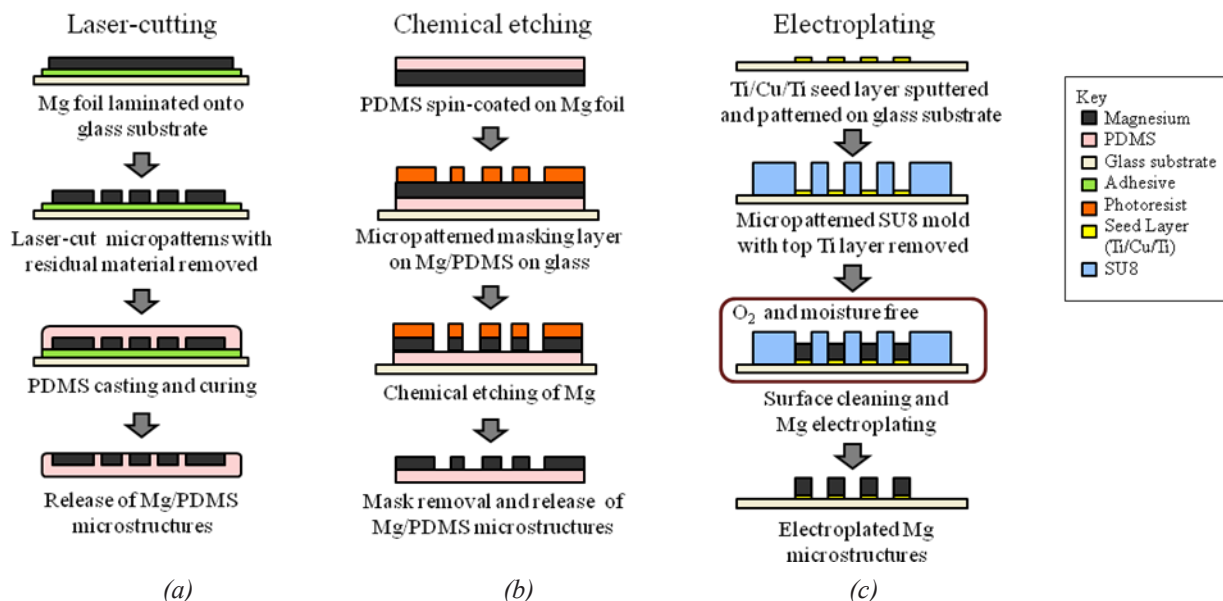


Figure 1: Fabrication schemes for the (a) laser-cutting, (b) chemical etching, and (c) electroplating of Mg microstructures.

## FABRICATION PROCESSES

### Laser Micromachining

Laser micromachining was investigated for the fabrication of high density, micron-scale magnesium microstructures and their integration into MEMS processes. Figure 1a presents the fabrication process for laser-cut magnesium microstructures embedded in polydimethylsiloxane (PDMS). Laser micromachining was performed on commercially-available 70- $\mu\text{m}$ -thick magnesium foil (99.9% pure) using an infrared laser (Resonetics, Nd:YLF, 1047 nm) operating at 180 ns pulses and a power density of  $18 \times 10^{12} \text{ W/m}^2$ . Prior to laser micromachining, magnesium foils were cleaned in 15% citric acid and laminated onto a glass substrate with adhesive. Samples were cut at a cutting velocity of 1 mm/s for 3 to 5 passes. Laser cutting conditions and post-processing treatment with citric acid have been optimized to minimize the amount of redeposited material onto the surfaces and sidewalls of the fabricated structures. The samples were then cast with 50- $\mu\text{m}$ -thick PDMS, and immersed in acetone to release the PDMS-embedded magnesium microstructures from the glass substrate, as described in Figure 1a.

### Chemical Etching

The chemical etching of magnesium was explored as a subtractive, batch-scale approach for the micropatterning of MEMS-relevant geometries. Improvement upon the previously-reported achievable feature sizes (i.e., width and spacing) would promote the use of chemical etching for the micropatterning of thick magnesium structures for MEMS. Figure 1b illustrates the fabrication process for the chemical etching of magnesium microstructures on PDMS substrates. Chemical etching was performed in a 1:50 solution of hydrochloric acid in deionized water and through a micropatterned photoresist mold. Commercial magnesium foils (70- $\mu\text{m}$ -thick) were cleaned with solvent and citric acid to remove surface residues and oxides. Prior to photoresist patterning, one side of the magnesium foils was spin-coated with PDMS and mounted onto a glass substrate to confine etching to the opposite side and to serve as a substrate for the etched structures. Planar circular coils were fabricated by the chemical etching of magnesium foil through a photoresist mask (Microposit S1813 positive resist) featuring 50- $\mu\text{m}$ -wide gaps and 250- $\mu\text{m}$ -wide lines. Etched samples were immersed in acetone to remove the photoresist mask and released from the underlying substrate.

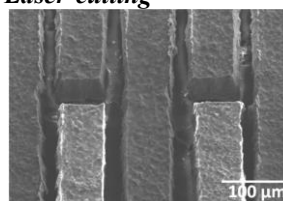
### Electroplating

The through-mold electrodeposition of magnesium was investigated to develop an additive approach for the micropatterning of thick magnesium films. In contrast to laser micromachining and chemical etching, the additive nature of electrodeposition enables the micropatterning of magnesium structures directly onto MEMS substrates. Electrodeposition also offers the ability to develop three-dimensional structures that cannot be achieved from foil-patterning technologies using multiple electroplating steps. Figure 1c describes the fabrication process for magnesium microstructures electroplated from non-aqueous solution. Magnesium electroplating from an aqueous solution is challenging because the potential

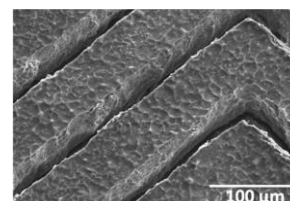
required for magnesium electrodeposition is less noble than its standard electrode potential against hydrogen [2]. As a result, the electrodeposition of magnesium was conducted from a non-aqueous 3 M solution of methylmagnesium chloride ( $\text{CH}_3\text{MgCl}$ ) in tetrahydrofuran (THF). The electroplating procedure was performed in a moisture-free glove box under inert argon atmosphere because the electrolyte solution is anhydrous and contains strong reducing agents. The measured temperature and relative humidity during electrodeposition were approximately 27°C and 7%, respectively.

Glass substrates were metalized (Ti/Cu/Ti) and the metals were chemically etched through a photoresist mask to provide a patterned seed layer. It was experimentally validated that photodefinable SU-8 epoxy is stable in THF solution over several hours. As a result, SU-8 was selected as the electroplating mold. The SU-8 was processed using the patterned seed layer as a photomask for reverse-side exposure [11]. The electroplating mold featured a width, spacing, and thickness of 50  $\mu\text{m}$ , 250  $\mu\text{m}$ , and 60  $\mu\text{m}$ , respectively. The surface protective layer of titanium was etched away in diluted hydrofluoric acid and samples were cleaned with salicylic acid solution prior to plating. Experiments using pulse plating conditions were conducted with an average current density of 15  $\text{mA/cm}^2$ . Plated samples were rinsed in anhydrous THF and vacuum dried. The SU-8 plating mold was removed using reactive ion etching (RIE) at a 1:10 ratio of trifluoromethane ( $\text{CHF}_3$ ) and oxygen ( $\text{O}_2$ ) at 150 mTorr and 300 W.

### Laser-cutting

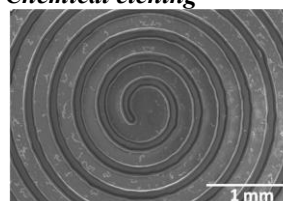


(a)

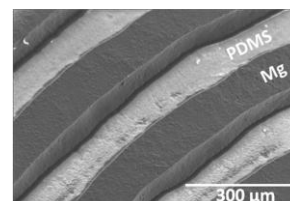


(b)

### Chemical etching

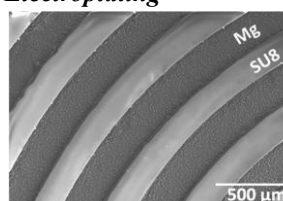


(c)

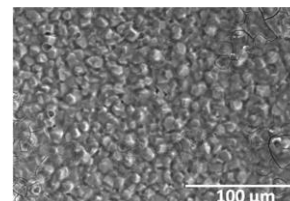


(d)

### Electroplating



(e)



(f)

Figure 2: Magnesium microstructures fabricated by (a, b) laser-cutting, (c, d) chemical etching, and (e, f) electroplating. EDX analysis showed that the atomic composition of the electroplated material was 89% magnesium and 11% oxygen. For comparison, EDX analysis of commercially-available Mg foil showed 90% magnesium and 10% oxygen.

## RESULTS & DISCUSSION

### Laser Micromachining

Planar spiral and interdigitated comb geometries fabricated from laser micromachining (Figure 2) featured a minimum line width and gap of 80  $\mu\text{m}$  and 20  $\mu\text{m}$ , respectively, with variations of  $\pm 5 \mu\text{m}$ . The surface roughness of the magnesium microstructures after post-process chemical treatment was less than 2  $\mu\text{m}$ . Laser-cutting conditions have been optimized to achieve the minimum gap, with higher cutting velocity and reduced power transmission corresponding to finer spacing. Limitations to achieving narrower gaps were the redeposition of debris and oxidation that occurs at the sidewall of laser-cut structures. Multiple passes were required to maintain a clear, continuous spacing between adjacent turns. Magnesium microstructures were treated with citric acid after laser-cutting to remove redeposited materials from the surface and sidewall. Although citric acid preferentially removes metal oxides (e.g., MgO), it will also etch magnesium isotropically via an oxidative mechanism [12]. Figure 3 presents a comparison of laser-cut microstructures before and after citric acid treatment. As shown, treatment with citric acid reduces the sidewall roughness attributed to redeposition. Measurements confirmed that this chemical treatment step also reduced the thickness by 15% and increased the overall surface roughness of the laser-cut magnesium microstructures by three-fold.

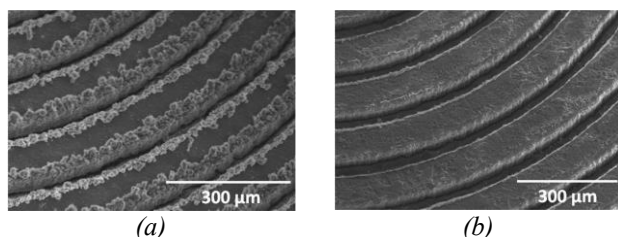


Figure 3: Laser-cut magnesium microstructures (a) before and (b) after treatment with citric acid to remove sidewall redeposition.

### Chemical Etching

Magnesium microstructures patterned by chemical etching featured line widths and gaps of 150  $\mu\text{m} \pm 10 \mu\text{m}$  (Figure 2). Structures etched with dilute hydrochloric acid demonstrated greater uniformity, with reduced undulations along the sidewalls and less surface roughness (<1  $\mu\text{m}$ ), than laser micromachined magnesium structures treated with citric acid. The magnesium microstructures fabricated using hydrochloric acid exhibited finer feature sizes than previously-reported results on the photochemical etching of magnesium with nitric acid [6].

Due to the isotropic nature of chemical etching, the fabricated structures were narrower than the designed patterns. Although the mask design may compensate for lateral etching, this strategy was limited by the challenge of etching through photomask features that were narrower than 30  $\mu\text{m}$  in width. However, it was measured that the extent of lateral etching was less than that of vertical etching. Specifically, the vertical etch rate of 70- $\mu\text{m}$ -thick magnesium micropatterns in 1:50 hydrochloric acid was 7.5  $\mu\text{m}/\text{min}$ , whereas the lateral etch rate was 5.5  $\mu\text{m}/\text{min}$ . Figure 4 shows the sloped sidewalls consistent with these etch rates, with greater undercut at the surface than the

bottom of the etched structure. The outermost features (i.e., outer turns of a planar coil) and sharp corners also etched faster than inner features, resulting in over-etching in the outer regions. Another limitation to chemical etching is its dependence on the starting quality of the commercial magnesium foil as small surface defects (e.g., debris, impurities, and micro-scratches) greatly affected the etching results.

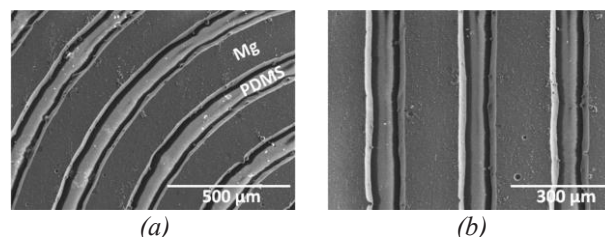


Figure 4: Magnesium microstructure chemically etched with 1:50 HCl:H<sub>2</sub>O. The difference in feature width between the bottom and top of the sample is caused by the isotropic nature of chemical etching.

### Electroplating

Test electroplated magnesium coils were 250  $\mu\text{m}$  wide with 50  $\mu\text{m}$  gaps between turns (Figure 2 e- f). Thicknesses ranging from 15  $\mu\text{m}$  to 50  $\mu\text{m}$  were achieved with a variation of  $\pm 5 \mu\text{m}$  observed across substrates. Energy-dispersive X-ray (EDX) analysis determined that the atomic composition at the surface of the electroplated material was 89% magnesium and 11% oxygen. EDX measurements further confirmed that reactive ion etching of the SU-8 mold did not affect the surface chemistry or morphology of the electroplated magnesium. For comparison, commercially available magnesium foil that was used for laser cutting and chemical etching comprises 90% magnesium and 10% oxygen.

The surface roughness of the electroplated magnesium was measured at approximately 3  $\mu\text{m}$ , as determined by confocal microscopy. Figures 2e-f show a magnesium coil electrodeposited under pulse current conditions ( $t_{\text{on}} = 0.2 \text{ ms}$ ,  $t_{\text{off}} = 0.8 \text{ ms}$ ; 20% duty cycle) at an average current density of 15  $\text{mA}/\text{cm}^2$ . The electrodeposition rate was approximately 8  $\mu\text{m}/\text{h}$ . The electroplated structure exhibited a thickness of  $15 \pm 3 \mu\text{m}$  and a grain size of approximately 10  $\mu\text{m}$ . As shown, the electroplated material featured coherent and dense packing in spite of the surface grain size. The surface morphology and grain size of the electroplated magnesium strongly depended on the plating conditions. The electrodeposition of magnesium was performed under pulse current conditions, as finer grains were achieved at lower duty cycles and shorter on-times.

Figure 5 shows the top and bottom surfaces of a magnesium coil electroplated at an average current density of 15  $\text{mA}/\text{cm}^2$  for a 20% duty cycle ( $t_{\text{on}} = 1 \text{ ms}$ ,  $t_{\text{off}} = 4 \text{ ms}$ ). The magnesium structure was embedded in PDMS and released from the glass substrate by peeling away the Mg-PDMS construct after heat treatment. Titanium and copper seed layers were chemically removed to reveal the bottom surface of the electroplated magnesium. The average thickness of the electroplated structure was  $50 \pm 5 \mu\text{m}$ . The top surface demonstrated a granular morphology, whereas the bottom surface was smooth with indistinguishable grains at the micron-scale. It was experimentally observed that for electroplated films

thicker than 15  $\mu\text{m}$ , lower duty cycle and current density resulted in greater uniformity of the through-mold electroplated magnesium. Specifically, this corresponded to less variation in the thickness and grain size of the magnesium from the center to the edge of the electroplated region. Preliminary results were limited to 50- $\mu\text{m}$ -thick structures, as thicker SU-8 molds tended to swell and delaminate with extended immersion in the plating solution.

Electrical characterization of the magnesium films and microstructures was performed using a conventional 4-point DC resistance measurement technique. The electrical resistivity of the plated magnesium was 8.7  $\mu\Omega\cdot\text{cm}$ . For comparison, the measured resistivity of commercially-available Mg foil was 5.3  $\mu\Omega\cdot\text{cm}$  and the reported resistivity of bulk magnesium is 4.4  $\mu\Omega\cdot\text{cm}$  [13]. Together, these results demonstrated that through-mold pulse electroplating provides a viable approach for the microfabrication of micron-thick and electrically continuous magnesium microstructures.

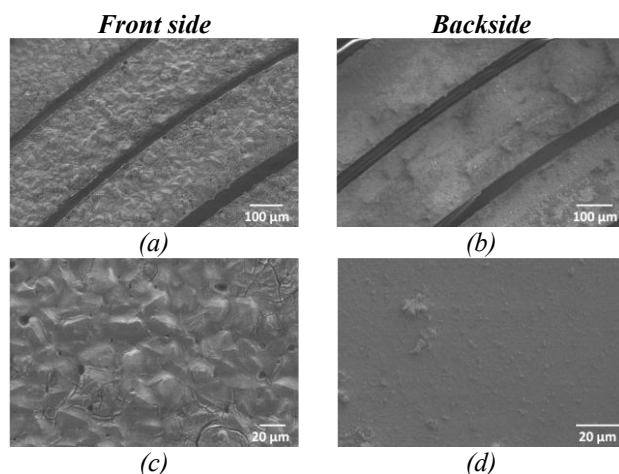


Figure 5: Electroplated magnesium planar spirals featuring a line width and spacing of 250  $\mu\text{m}$  and 50  $\mu\text{m}$ , respectively. (a, c) Front side and (b, d) backside of magnesium microstructures after RIE removal of the SU-8 electroplating mold.

#### Comparison of Mg fabrication processes

This study investigated three approaches to the microfabrication of magnesium. Laser cutting and chemical etching represented subtractive approaches to the micropatterning of magnesium. Laser cutting demonstrated the smallest feature size within the scope of this work and, in comparison to chemical etching, is amenable to sharp (i.e., non-rounded) features. Although chemical cleaning was required to remove redeposited material, gaps as narrow as 20  $\mu\text{m}$  were achieved using laser micromachining techniques in 70- $\mu\text{m}$ -thick magnesium films. Chemical etching with dilute hydrochloric acid provided a batch process for the micropatterning of magnesium with smooth, sloped sidewalls. The outermost regions and non-rounded features of the fabricated microstructures etched more quickly. However, the chemically etched microstructures exhibited line widths and spacing of approximately 150  $\mu\text{m}$ , demonstrating finer feature sizes than previously-reported results with nitric acid.

Through-mold electroplating provided an additive approach for magnesium micropatterning at thicknesses that exceed what is achievable with sputtering and evaporation. In contrast to laser-cutting and chemical etching, through-mold electroplating provides magnesium microstructures with smooth, vertical side walls. Further, the additive approach of electroplating promotes the microfabrication of non-planar microstructures with magnesium. The minimum feature size is limited by the lithographic patterning of the electroplating mold and by the grain size of the plated material. However, grain size and surface morphology may be controlled by the electroplating parameters and electrolyte composition. As the electrodeposition takes place from a non-aqueous solution, negative photoresists commonly used for electroplating molds were incompatible with this approach. The mold material must withstand long-term immersion in a solvent without solubilizing or substantial swelling. In addition, the electroplating process must take place in an oxygen- and moisture- free environment.

## CONCLUSIONS

This study demonstrated that magnesium microstructures of dimensions relevant to MEMS can be achieved through laser micromachining, chemical etching, and through-mold electroplating technologies. The fabrication processes provide additive and subtractive approaches to magnesium micropatterning at thicknesses in the tens of microns range. Further, the magnesium microstructures were fabricated on MEMS-compatible substrates, embedded in PDMS and subsequently released to demonstrate the ability of integrating these magnesium microfabrication technologies with other MEMS. Magnesium exhibits favorable electrochemical and mechanical properties, and the development of magnesium microfabrication technologies will promote the use of this unique element in applications ranging from high energy density batteries to biodegradable MEMS implants.

## REFERENCES

- [1] P.E. DeGarmo, *Materials and processes in manufacturing*, Collin Macmillan (1979).
- [2] T.D. Gregory, *et al.*, *J. Electrochem. Soc.*, 137 (1990).
- [3] M. Morajev and D. Mantovani, *Int. J. Mol. Sci.*, 12 (2011).
- [4] M.H. Lee, *et al.*, *Surf. Coat. Tech.*, 169-170 (2003).
- [5] S.W. Hwang, *et al.*, *Science*, 337 (2012).
- [6] D.M. Allen, *et al.*, *J. Micromech. Microeng.*, 20 (2010).
- [7] C.M. Boutry, *et al.*, *Procedia Engineering*, 25 (2011).
- [8] R.J. Gummow and Y. He, *J. Electrochem. Soc.*, 157 (2010).
- [9] S.P. Davis, *et al.*, *Transducers Tech. Digest*, pp. 1435-38 (2007).
- [10] A.B. Frazier and M.G. Allen, *J. Microelectromech. Sys.*, 6 (1997).
- [11] Y.K. Yoon and M.G. Allen, *53<sup>rd</sup> Electronic Components and Technology Conference*, pp. 1534-40 (2003).
- [12] H.K. DeLong, *USPO*, 2,302,939.
- [13] T.C. Chi, *J. Phys. Chem. Ref. Data*, 8 (1979).

## CONTACT

M. Tsang, tel: +1-404-894-5251; [mtsang7@gatech.edu](mailto:mtsang7@gatech.edu)